Planet. Space Sci. 1968, Vol. 16, pp. 587 to 605. Pergamon Press. Printed in Northern Ireland

THE HYDROMAGNETIC STABILITY OF THE MAGNETOSPHERIC BOUNDARY

D. J. SOUTHWOOD
Imperial College, Department of Physics, London

(*Received* 29 *November* 1967)

Abstract—The hydromagnetic Kelvin–Helmholtz stability problem is studied for an infinite plane interface between compressible infinitely conducting fluids. The critical value of the relative streaming velocity for stability is studied by use of the equations for marginal stability without making the simplifying physical assumptions used by previous authors.

In application to the magnetosphere boundary we find we can make some predictions without too precise a knowledge of all the parameters involved. At middle and low latitudes the first growing modes propagate across the Earth's field with a very low phase velocity and wave fronts closely aligned to meridian planes. The modes tend to exhibit circular polarisation in a plane almost perpendicular to the Earth's field. This behaviour should also occur at high latitudes when the magnetosheath field is closely aligned to he Earth's field.

INTRODUCTION

In this paper we study the stability problem of the hydromagnetic Kelvin–Helmholtz model of the intervace. Many authors have studied this problem previously; most recently Fejer (1964), Sen (1965) and Lerche (1966). Due to the complex nature of the dispersion relation Fejer and Sen both introduce simplifying assumptions which do not seem valid for the magnetosphere (e.g. identical acoustic and magnetic field properties on either side of the boundary) Sen finds the most unstable perturbation is that propagating perpendicular to the unperturbed magnetic field; while Fejer, in the cases he studies, finds the first unstable modes propagate parallel to the streaming velocity. The relationship between these findings should be shown to some extent in the more general treatment given here.

Lerche deduces from the dispersion relation that the stability criterion depends on the phase velocity of the particular modes and points out that therefore the highest growth rate occurs for the shortest wavelengths in the hydromagnetic approximation. He argues then that for wavelengths with significant growth rates Landau damping might also be significant. While accepting that this is a drawback inherent in any MHD treatment of the problem we would maintain it should still be regarded as a necessary preliminary for a fuller study of the boundary problem. One might expect a situation analogous to that of wind driven waves on water where since non-linear effects set in when the amplitude is comparable to the wave length one can expect longer wavelengths predominating further away from the point where growing waves first occur c.f. Dungey (1967a).

THE MODEL

We then take as our model a Kelvin–Helmholtz discontinuity between two compressible infinitely conducting fluids. As in previous treatments we will neglect curvature of field lines. The boundary layer will be considered to have negligible thickness. This and the MHD assumption clearly place lower limits on the allowable wavelengths for boundary disturbances. The assumption of infinite conductivity and the consequent expression for the electric field

$$\mathbf{E} = -\mathbf{u} \times \mathbf{B},$$

where **u** is the fluid velocity place the condition on the magnetic fields on either side of the boundary of being tangential to the boundary. (Requirement of continuity of tangential electric field gives this immediately).

We will consider the plasma on each side of the interface in its own rest frame first and then link the behaviour on each side by use of the required boundary conditions.

EQUATIONS OF MOTION

In linearised form, denoting first order perturbations by suffices (1) we have (1) the equation of motion, (2) the flux equation and (3) the equation of continuity.

$$\rho \frac{\partial \mathbf{v}^{(1)}}{\partial t} = -\nabla p^{(1)} + \frac{1}{\mu} \operatorname{curl} \mathbf{B}^{(1)} \times \mathbf{B}, \tag{1}$$

$$\operatorname{curl} (\mathbf{v}^{(1)} \times \mathbf{B}) = \frac{\partial \mathbf{B}^{(1)}}{\partial t}, \tag{2}$$

$$\frac{\partial \rho^{(1)}}{\partial t} = -\rho \operatorname{div} \mathbf{v}^{(1)}. \tag{3}$$

Unsuffixed letters, refer to the original unperturbed quantities which we assume to be locally constant in space and time.

Assuming now all perturbed quantities vary as exp. $\{i(\mathbf{k} \cdot \mathbf{r} - \omega t)\}$, ω being the frequency in the rest frame of each side, we can derive the well-known dispersion relation

$$\omega^4 - \omega^2 k^2 (c^2 + \mathbf{A}^2) + k^2 c^2 (\mathbf{k} \cdot \mathbf{A})^2 = 0, \tag{4}$$

where c and **A** are the sound speed and the vectorial Alfven velocity defined respectively by

$$p^{(1)} = c^2 \rho^{(1)} \quad \text{and} \quad \mathbf{A} = \frac{\mathbf{B}}{\sqrt{\mu \rho}}. \tag{5}$$

BOUNDARY REQUIREMENTS AND DISPERSION RELATION

We now write $\mathbf{k} = \mathbf{k}_t + \hat{\mathbf{n}} k_n$ where k_t is component of **k** parallel to the interface and $\hat{\mathbf{n}}$ is a unit vector normal to the interface directed into the plasma under consideration.

From the physical requirement that disturbances should not grow in space away from the interface we impose the condition (6)

$$I(k_n) > 0. \tag{6}$$

This requires we use coordinate systems on either side such that **r** is measured positive increasing away from the boundary. We can rewrite (4) now as

$$\omega^4 - \omega^2 (k_t^2 + k_n^2)(c^2 + \mathbf{A}^2) + c^2 (\mathbf{k}_t \cdot \mathbf{A})(k_t^2 + k_n^2) = 0 \tag{7}$$

having used the fact that **B** is tangential to the boundary.

We may put this in dimensionless form by writing

$$x = \frac{\omega}{k_t A}, a = \frac{c}{A}, y = \frac{k_n}{k_t}, \cos\theta = \frac{\mathbf{k}_t \cdot \mathbf{A}}{k_t A}. \tag{8}$$

θ then is the angle between the tangential propagation vector and the magnetic field.

(7) then becomes

$$x^4 - x^2 (1 + a^2)(1 + y^2) + (1 + y^2) a^2 \cos^2\theta = 0,$$

which after a little algebra, solving for y, gives

$$y = \left\{\frac{x^4 - (1 + a^2)x^2 + a^2 \cos^2\theta}{x^2(1 + a^2) - a^2 \cos^2\theta}\right\}^{1/2} = \left\{\frac{(x^2 - x^{(f)^2})(x^2 - x^{(s)^2})}{x^2(1 + a^2) - a^2 \cos^2\theta}\right\}^{1/2} \tag{9}$$

where

$$x^{(f)} = \frac{V^{(f)}}{A} \qquad \text{and} \qquad x^{(s)} = \frac{V^{(s)}}{A}$$

$V^{(f)}$, $V^{(s)}$ being the phase velocities of the fast and slow modes propagating parallel to $\mathbf{k}_t$ into a compressible media.

The two hydromagnetic boundary conditions we shall use are that there is no cavitation and that hydromagnetic stress is balanced on each side in both perturbed and unperturbed states.

If δr is the displacement perpendicular to the interface, we have that

$$\delta r_1 = -\delta r_2 \tag{10}$$

using subscripts to label sides of the boundary.

In the unperturbed state a pressure balance is required across the interface, so

$$p_1 + \frac{B_1^2}{2\mu} = p_2 + \frac{B_2^2}{2\mu} \tag{11}$$

where also

$$p + \frac{B^2}{2\mu} = \rho(\gamma^{-1}c^2 + \tfrac{1}{2}A^2) \tag{12}$$

assuming the adiabatic condition

$$p = \rho^{\gamma}.$$

In the perturbed state the stress associated with the disturbance must be equal on each side. To find an expression for this stress we consider the component of the fluid equation of motion perpendicular to the interface.

Writing (2) in the form

$$\omega\mathbf{B}^{(1)} = -\mathbf{k} \times (\mathbf{v}^{(1)} \times \mathbf{B}) = (\mathbf{k} \cdot \mathbf{v}^{(1)})\mathbf{B} - (\mathbf{B} \cdot \mathbf{k}_t)\mathbf{v}^{(1)} \tag{2a}$$

and writing (1) as

$$-\rho\omega\mathbf{v} = -\mathbf{k}p^{(1)} + \frac{1}{\mu}(\mathbf{k} \times \mathbf{B}^{(1)}) \times \mathbf{B} = -\mathbf{k}\left(p^{(1)} + \frac{\mathbf{B} \cdot \mathbf{B}^{(1)}}{\mu}\right) + \frac{\mathbf{B} \cdot \mathbf{k}_t}{\mu}\mathbf{B}^{(1)} \tag{1a}$$

using (2a) and taking the component normal to the boundary we find

$$\begin{aligned} p^{(1)} + \frac{\mathbf{B} \cdot \mathbf{B}^{(1)}}{\mu} &= \frac{1}{k_n}\left(\rho\omega^2 - \frac{(\mathbf{B} \cdot \mathbf{k}_t)^2}{\mu}\right)\delta r \\ &= \frac{\rho}{k_n}(\omega^2 - A_2 k_t^2 \cos^2\theta)\,\delta r \\ &= \frac{\rho A^2 k_t}{y}(x^2 - \cos^2\theta)\,\delta r \qquad \text{using (8)} \end{aligned}$$

from (12)

$$\frac{\rho_1 A_1^2}{\rho_2 A_2^2} = \frac{(\frac{3}{5}a_2^2 + \frac{1}{2})}{(\frac{3}{5}a_1^2 + \frac{1}{2})}$$

so using (10) at the boundary

$$R(x) = \frac{(x^2 - \cos^2\theta)}{(\frac{8}{5}a^2 + 1)y}$$

is such that

$$R_1(x_1) = -R_2(x_2) \tag{13}$$

(13) is in effect the dispersion relation together with (9) and a particular value of the streaming speed U. This is found by requiring the frequency of the disturbances in any arbitrary frame to be the same on either side. Therefore

$$\omega_1 - \mathbf{B} \cdot \mathbf{k}_t = \omega_2.$$

Writing ϕ as the angle between $\mathbf{k}_t$ and $\mathbf{U}$, we have

$$U \cos\phi = \frac{\omega_1}{k_t} - \frac{\omega_2}{k_t}. \tag{14}$$

Physically, since we expect (and in fact will show) the waves to go the same way as the wind they see, we take ω_2/k_t to be negative if we take the rest frame on side one as our frame of

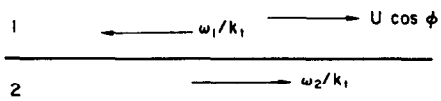

FIG. 1. RELATIVE DIRECTIONS OF TANGENTIAL PHASE VELOCITIES IN THE FRAME OF THE PLASMA ON SIDE 2.

reference (c.f. Fig. 1). We therefore write

$$\frac{\omega_2}{k_t A_2} = -x_2.$$

(14) then gives

$$U \cos\phi = A_1 x_1 + A_2 x_2 \tag{14a}$$

and (13) becomes

$$R_1(x_1) = -R_2(-x_2). \tag{13a}$$

MARGINAL STABILITY

Using Equations (13a) for a given real value of x, it is possible in principle to find corresponding values of x_2 and, by use of (14a), the corresponding value of the component of streaming velocity may be found.

In general for a given value of U and ϕ by substitution into (13a) from (14a) one obtains a tenth order equation in x_1 or x_2. The roots of this equation will be real or occur in complex conjugate pairs and not all will be allowable due to the physical requirement, (6). If a root occurs with a positive imaginary part and also satisfies (6), we have instability. When $U = 0$ we have a stable situation; for some value of $U \cos\phi > 0$ the first allowable roots of (13a) with positive imaginary parts will occur. This will mark the transition from stable to unstable hydromagnetic flow.

We find the critical value of $U \cos\phi$ allowing x_1 and x_2 small positive imaginary parts ε_1, ε_2 and expand (13a) in a Taylor expansion to first order in ε. This is equivalent to looking for coincident roots in the tenth order equation previously mentioned. ε_1 and ε_2

are related by the requirement of an equal growth rate on either side
Therefore

$$k_t A_1 \varepsilon_1 = k_t A_2 \varepsilon_2,$$

i.e.

$$\frac{\varepsilon_1}{\varepsilon_2} = \frac{A_2}{A_1}. \tag{15}$$

Now

$$R(x + i\varepsilon) = R(x) + i\varepsilon \frac{\mathrm{d}R}{\mathrm{d}x}(x) + O(\varepsilon^2)$$

and also

$$y(x + i\varepsilon) = y(x) + i\varepsilon \frac{\mathrm{d}y}{\mathrm{d}x}(x) + O(\varepsilon^2).$$

We may now plot $y_1(x_1 + i\varepsilon_1)$ schematically on an Argand diagram as in Fig. 2 using only the sign of $\mathrm{d}y/\mathrm{d}x$ and requirement (6). $y_2(-x_2 + i\varepsilon_2)$ on such a schematic plot is purely a mirror image of $y_1(x_1 + i\varepsilon_1)$. We can make a similar plot $R_1(x_1 + i\varepsilon_1)$ as in Fig. 3. Similarly $R_2(-x_2 + i\varepsilon_2)$ is also a mirror image schematically. The superposition of the plots of $R_1(x_1 + i\varepsilon_1)$ and $-R_2(-x_2 + i\varepsilon_2)$ in Fig. 4 shows we may pick out the regimes of x_1, x_2 where crossing points may occur. On this figure on the contour R_2 values of x_2 at the end points of sections of the contour on which possible intersections with parts of the R_1 contour occur, have been marked. These are

$$x_2 = 0,\ \alpha_2,\ \beta_2,\ x_2^{(s)},\ |\cos\theta_2|,\ \xi_2,\ x_2^{(f)}, \text{ and } X_2$$

where $x_2^{(f)}$, $x_2^{(s)}$, $|\cos\theta_2|$ have already been defined. We define

$$\alpha_2 = \frac{a_2}{\sqrt{(1 + a_2^2)}} = \alpha_2^0\,|\cos\theta_2| \text{ say.} \tag{16}$$

X_2 is defined by

$$\frac{\mathrm{d}R_2}{\mathrm{d}x_2}(X_2) = 0 \qquad X_2 > x_2^{(f)}.$$

$$\beta_2 \text{ by } -R(-\beta_2) = R_1(X_1) = R_2(\beta_2).$$

$$\xi_2 \text{ by } -R_2(-\xi_2) = R_1(0) = -R_2(\xi_2). \tag{17}$$

α_1, β_1, ξ_1, X_1, are defined similarly.

It is clear from this diagram that we require ω_1/k_t and ω_2/k_t to have different signs for growing modes to appear since plots of $R_1(x_1 + i\varepsilon_1)$ and $R_2(x_2 + i\varepsilon_2)$ subject to (6) would be entirely on opposite sides of the imaginary axis.

We can now by study of Fig. 4 mark off the only areas in the (x_1, x_2) plane in which intersections can occur as in Fig. 5.

To find the critical value of U for marginal stability we have to use

$$U\cos\phi = A_1 x_1 + A_2 x_2.$$

On Fig. 5 this is represented by a line of slope $-A_1/A_2$. At $U = 0$, the origin, we have a stable situation, therefore instability can only begin when we have increased U such that $A_1 x_1 + A_2 x_2 = U\cos\phi$ intersects with one of the hatched areas (treating ϕ for the moment

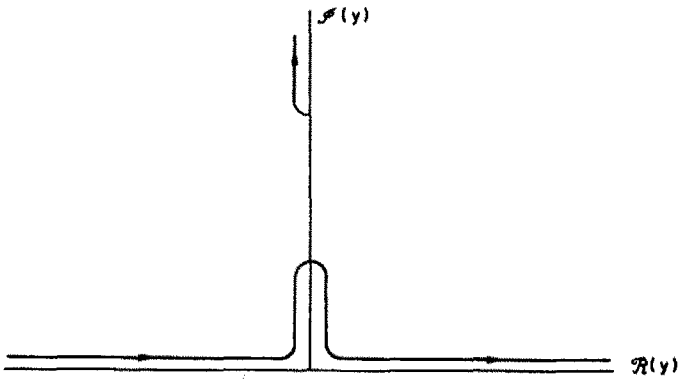

FIG. 2. SCHEMATIC ARGAND PLOT OF $y(x + i\epsilon)$ AS x VARIES FROM 0 TO ∞ WITH THE RESTRICTION $I(y) > 0$.

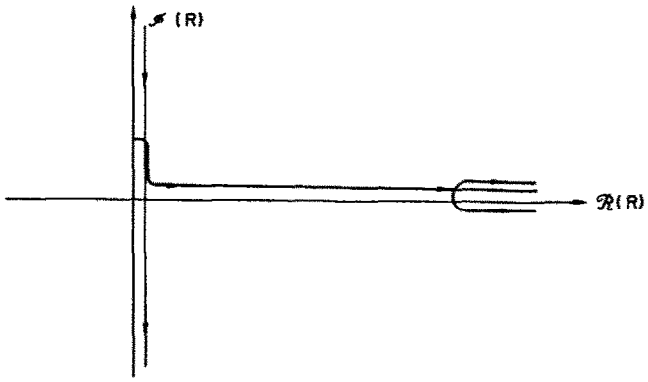

FIG. 3. SCHEMATIC PLOTS OF $R(x + i\epsilon)$ AS x VARIES FROM 0 TO ∞.

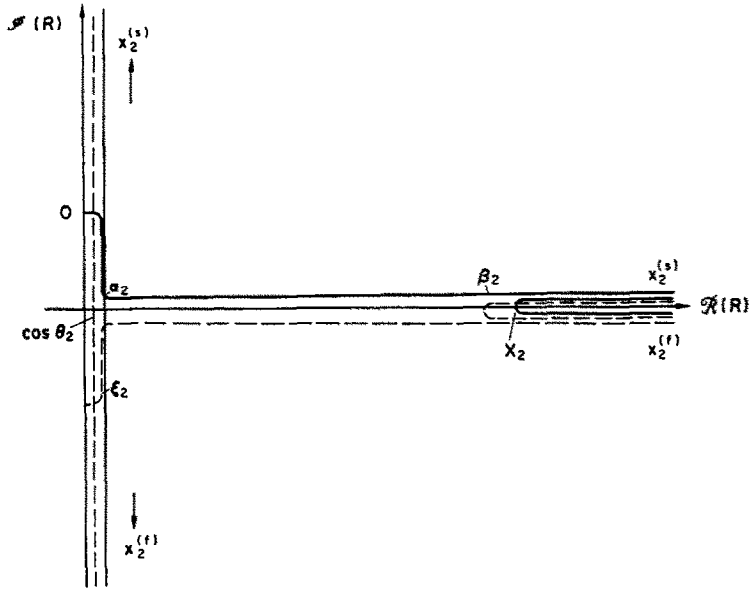

FIG. 4. SUPERPOSED PLOTS OF R_1 AND $-R_2$ MARKING CRITICAL VALUES OF x_2 ON R_2.

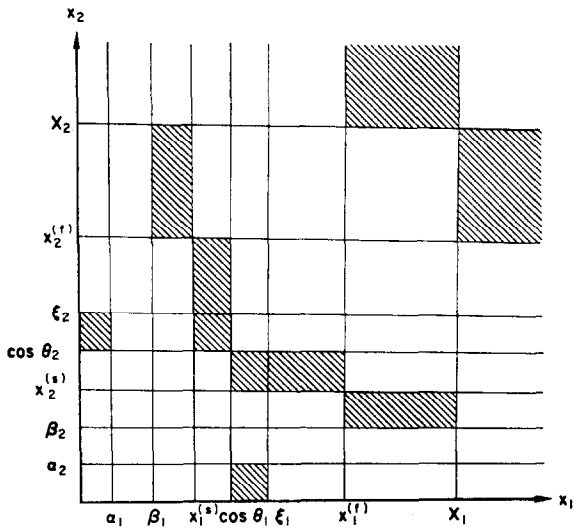

FIG. 5. AREAS IN THE (x_1, x_2) PLANE WHERE MARGINAL STABILITY REQUIREMENTS COULD BE SATISFIED.

as a constant). From Fig. 5, then it is clear that the two particular areas of interest are the two areas bounded by

$$x_i = |\cos\theta_i|, \xi_i \qquad i = 1, j = 2$$

$$x_j = 0, \alpha_j \qquad i = 2, j = 1.$$

In these areas we are interested in points where

$$R_1(x_1 + i\varepsilon_1) = -R_2(-x_2 + i\varepsilon_2).$$

$R_1(x_1)$ and $R_2(x_2)$ are imaginary in these areas; we therefore require points where

$$R_1(x_1) = -R_2(x_2) \tag{18}$$

$$\varepsilon_1 \frac{\mathrm{d}R_1(x_1)}{\mathrm{d}x_1} = \varepsilon_2 \frac{\mathrm{d}R_2(x_2)}{\mathrm{d}x_2}. \tag{19}$$

Using (15), (19) becomes

$$\frac{A_1}{A_2} = \frac{\mathrm{d}R_1/\mathrm{d}x_1}{\mathrm{d}R_2/\mathrm{d}x_2}. \tag{20}$$

Points of intersection will lie on a curve in the (x_1, x_2) plane defined by

$$F(x_1, x_2) = (R_1(x_1) + R_2(x_2)) = 0. \tag{21}$$

The function is continuous in the areas we are considering, therefore since

$$\mathrm{d}F = \frac{\mathrm{d}}{\mathrm{d}x_1} R_1(x_1)\,\mathrm{d}x_1 + \frac{\mathrm{d}}{\mathrm{d}x_2} R_2(x_2)\,\mathrm{d}x_2 = 0$$

$$\frac{\mathrm{d}x_2}{\mathrm{d}x_1} = -\frac{\mathrm{d}R_1(x_1)/\mathrm{d}x_1}{\mathrm{d}R_2(x_2)/\mathrm{d}x_2} \tag{22}$$

Now the slope of

$$A_1x_1 + A_2x_2 = U\cos\phi \text{ is } -A_1/A_2. \tag{23}$$

Therefore U may only increase until $A_1x_1 + A_2x_2 = U\cos\phi$ is tangential by virtue of (20), (22), and (23).
Since at

$$x_1 = \xi_1, \frac{dR_2}{dx_2} = 0$$

$$\frac{dx_2}{dx_1} \to -\infty$$

and at

$$x_1 = \cos\theta_1, \frac{dR_2}{dx_2} \to +\infty$$

therefore

$$\frac{dx_2}{dx_1} \to 0$$

for all values of A_1/A_2 there are points on $F(x_1, x_2) = 0$ such that marginal stability occurs for some values of U (see Fig. 6). Unfortunately the problem of finding how many roots

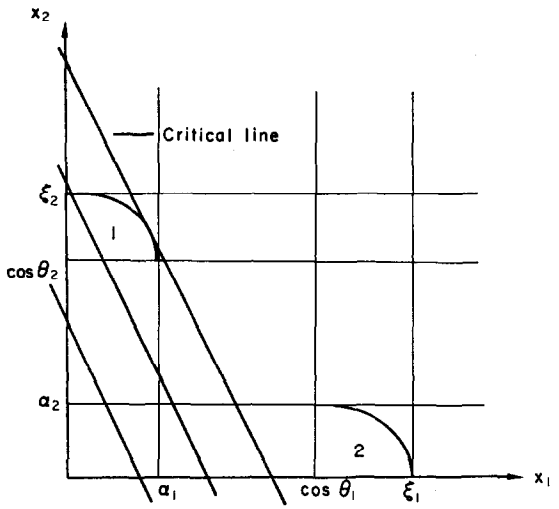

FIG. 6. DIAGRAM SHOWING LINES OF SLOPE $-A_1/A_2$ FOR INCREASING $U\cos\phi$.

there are in section 1 or 2 of Fig. 6 for given A_1/A_2 and varying U is rather intractable, so it should be stressed Fig. 6 is purely schematic.

STABILITY TO ALL MODES

As yet we have only considered propagation in a particular direction with respect to the magnetic fields and the streaming velocity. Since the most useful stability criterion from physical considerations is that to all modes we must be prepared to consider modes propagating in any direction for a given orientation of fields and stream velocity. We then write:

$$\theta_1 = \phi + \chi_1 \qquad \theta_2 = \phi + \chi_2, \tag{24}$$

where χ_1, χ_2 are the angles between $\mathbf{B}_1$, $\mathbf{B}_2$ and $\mathbf{U}$ respectively. We consider ϕ varying between 0° and 360°, giving us all possible direction of propagation. For the system to be stable we require that, for no value of ϕ, for a given value of U, do unstable modes exist.

We define critical values of x_1, x_2 for a particular direction as $\bar{x}_1(\phi)$, $\bar{x}_2(\phi)$. $\bar{x}_1$, $\bar{x}_2$ are then the simultaneous roots of (18) and (20) such that $A_1\bar{x}_1 + A_2\bar{x}_2$ is the minimum possible. The point $(\bar{x}_1, \bar{x}_2)$ will lie in either section 1 or 2 of Fig. 6 for each value of ϕ.

Our stability criterion is

$$U \cos \phi < V_1\bar{x}_1(\phi) + A_2\bar{x}_2(\phi) \tag{25}$$

for all values of ϕ.

If we write

$$\tilde{U}(\phi) = A_1\bar{x}_1(\phi) + A_2\bar{x}_2(\phi),$$

then the critical streaming velocity U_c for transition from a stable to unstable flow is given by

$$|U_c \cos \phi| = \tilde{U}(\phi)$$

for two particular values of ϕ between 0° and 360°. (The fact that 2 values of ϕ will arise is due to $\tilde{U}(\phi)$ having a period 180° in ϕ. This is clear from the nature of the dispersion relation.)

We can tackle the problem then by solving (18) and (20) for ϕ varying from 0° to 360° then making a polar plot of $\tilde{U}(\phi) = A_1\bar{x}_1(\phi) + A_2\bar{x}_2(\phi)$.

Stability can be tested for any value of U by plotting the circle $U \cos \phi$ on the same plot. If the plot of $U(\phi)$ completely encloses the plot of $U \cos \phi$ we have stability. The critical value of U, U_c, is found by finding the plot which is wholly enclosed by $\tilde{U}(\phi)$ but touches it.

Solving (18) and (20) algebraically is not possible, without simplifying assumptions which destroy important features of the problem, so we chose numerical values for quantities involved which seemed more reaonable than those used before for the magnetosphere. We took

$$\frac{A_1}{A_2} = 4 \qquad \frac{B_1}{B_2} = 1{\cdot}8 \qquad a_1 = \frac{c_1}{A_1} = \sqrt{\frac{1}{3}}$$

these requiring

$$a_2 = \frac{c_2}{A_2} = \frac{\sqrt{53}}{\sqrt{18}}.$$

We then plotted $\tilde{U}(\phi)$ for $\chi_1 - \chi_2 = 30°, 80°, 90°$.

It should be noted that to plot $U(\phi)$ one need not designate anything about the streaming velocity. One uses the physical conditions on either side and the relative orientation of the magnetic fields. With this plot one can then test for stability any value of U in any direction relative to the magnetic fields. Effectively after obtaining $\tilde{U}(\phi)$ one has yet to fix U or either χ_1 or χ_2.

NUMERICAL RESULTS AND SUGGESTED ANALYTIC CRITERION

The plots of $\tilde{U}(\phi)$ or rather $\tilde{U}/A_2$ in dimensionless form appear in Figs. 7–9. In Fig. 7 a plot is shown of $U_c \cos \phi/A_2$ for $\chi_1 = 32°$ $\chi_2 = 122°$. The recurrent feature in these plots is the cusp which occurs on the radius vector perpendicular to the largest field A_1. Provided the direction of the streaming velocity is not too closely aligned to the larger magnetic field we can expect the circular plot of $U_c \cos \phi/A_2$ to touch $\tilde{U}(\phi)/A_2$ at this cusp in the cases we have here. This means that unstable modes would first propagate in directions almost perpendicular to A_1.

This cusp is expected analytically since it corresponds to $\theta_1 = 90°$ in Fig. 6. Section 1 disappears entirely at this value of θ_1. As χ_1 tends to 90° section 1 exists and the point where

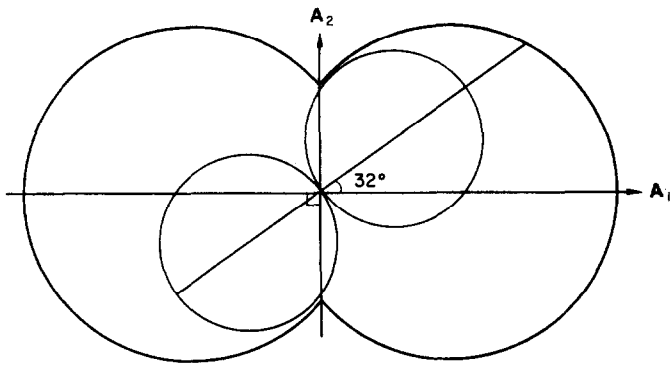

FIG. 7. COMPUTED PLOT OF $\tilde{U}/A_2$ FOR $\chi_1 - \chi_2 = 90°$, $A_1/A_2 = 4$, SHOWING TEST PLOT OF $U_c/A_2 \cos\phi$ FOR $\chi_1 = 32°$.

$A_1x_1 + A_2x_2 = U\cos\phi$ is tangential comes arbritrarily close to $(0, \cos\theta_2)$ in Fig. 8. Therefore if the orientation of magnetic fields and streaming velocity is such that U_c is defined by this cusp, since ϕ at this point is $90° - \chi_1$

$$U_c = \left|\frac{A_2 \cos(90° - \chi_1 + \chi_2)}{\cos(90° - \chi_1)}\right| = \left|\frac{A_2 \sin(\chi_1 - \chi_2)}{\sin\chi_1}\right|. \tag{26}$$

It is apparent from Figs. 7–9 when χ_1 is large this defines the critical streaming velocity. Also, when $\chi_1 - \chi_2$ is small, we can expect U_c to be defined by (26) for nearly all values of χ_1 save when U and A_1 are very closely aligned c.f. Fig. 9.

The critical streaming speed given by (26) would then seem to be applicable in many cases, but it would be useful to have some form of criterion to estimate when it comes into doubt.

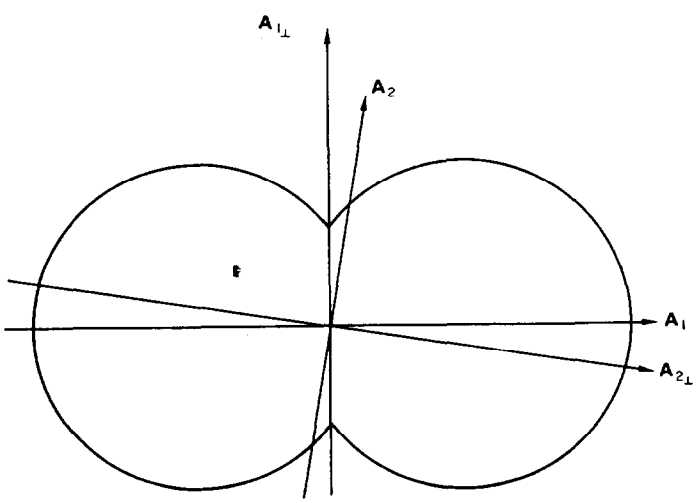

FIG. 8. COMPUTED PLOT OF $\tilde{U}/A_2$ FOR $\chi_1 - \chi_2 = 80°$, $A_1/A_2 = 4$.

In fact, it seems by comparison with the numerical plots one can assume

$$r(\phi) = \alpha_1{}^0 A_1 |\cos(\phi + \chi_1)| + A_2 |\cos(\phi + \chi_1)|$$

(i.e. the plot using the corner point of section 1 as an estimate of $\bar{x}_1, \bar{x}_2$) is a lower bound for $\tilde{U}(\phi)$ when $\bar{x}_1\ \bar{x}_2$ is on section 1. The justification for such an assumption is given in the

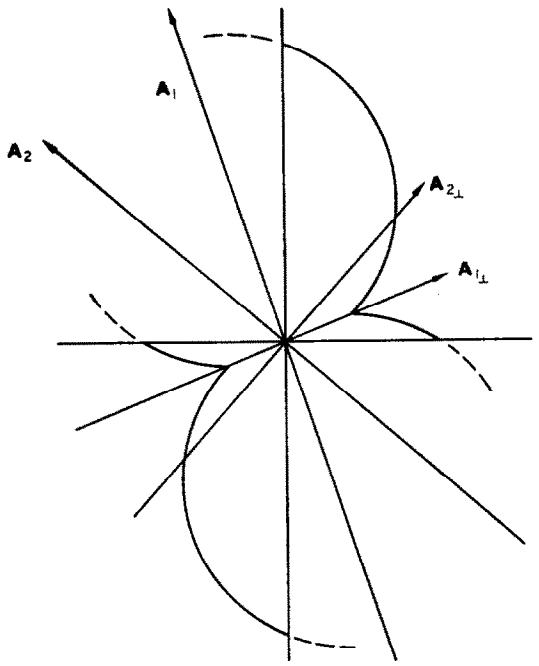

FIG. 9. COMPUTED PLOT OF $\tilde{U}/A_2$ NEAR $\theta_1 = 90°$ FOR $\chi_1 - \chi_2 = 30°$.

appendix to this paper. $r(\phi)$ has cusps on $\phi = 90 - \chi_1$ and $\phi = 90 - \chi_2$ and from its sinusoidal nature must intersect with any family of circles

$$r = \frac{U}{A_2} \cos\phi$$

with U increasing, first at these cusps. Intersection with the cusp on $\phi = 90 - \chi_1$ gives

$$U = \left| \frac{A_2 \sin(\chi_1 - \chi_2)}{\sin \chi_2} \right| \tag{27}$$

and with the cusp on $\phi = 90 - \chi_2$ gives

$$U = \left| \frac{\alpha_1{}^0 A_1 \sin(\chi_1 - \chi_2)}{\sin \chi_2} \right|.$$

(27) and (26) are identical so we suggest (26) comes into doubt when

$$\left| \frac{\alpha_1{}^0 A_1 \sin(\chi_1 - \chi_2)}{\sin \chi_2} \right| < \left| \frac{A_2 \sin(\chi_1 - \chi_2)}{\sin \chi_1} \right|,$$

or

$$|\alpha_1{}^0 A_1 \sin \chi_1| < |A_2 \sin \chi_2| \tag{28}$$

This in fact is more than adequate in the numerical cases we have computed but should be treated with caution when A_1, A_2 are of more comparable magnitude for reasons given in the next section.

QUALITATIVE DESCRIPTION OF VARIATIONS IN A_1/A_2

Analysis of the effect of variations in a_1, a_2, the ratio of sound speed to Alfven speed on either side has been done by Sen but the effect of varying A_1/A_2, the ratio of Alfven speeds across the boundary has not been studied before. This ratio is in fact very important. It is due to the fact that $A_1/A_2 > 1$ that the cusp on $\bar{U}(\phi)$ occurs with its associated conclusion that wave fronts for the first unstable modes are nearly perpendicular to the larger field.

When A_1/A_2 becomes infinite we can be sure that

$$A_1 x_1 + A_2 x_2 = U \cos \phi$$

as U increases will be tangential to section 1 in Fig. 6 prior to section 2 for all values of θ_1, θ_2 as ϕ varies. Obviously when A_1/A_2 is small, section 2 contains $(\bar{x}_1, \bar{x}_2)$. In the numerically computed case we took $A_1/A_2 = 4$ and as might be expected $(\bar{x}_1, \bar{x}_2)$ remained on 1. As we take A_1/A_2 closer to unity we can expect $\bar{U}(\phi)$ to take on a more symmetrical behaviour with respect to A_1, A_2 and consequently we may expect $(\bar{x}_1, \bar{x}_2)$ to change from 1 to 2 as ϕ varies. When $\chi_1 - \chi_2$ is small we can expect cusps in $\bar{U}(\phi)$ perpendicular to both A_1 and A_2 with two stability criteria like (26), being chosen, and when $\chi_1 - \chi_2 \sim 90$ we can expect $\bar{U}(\phi)$ to be more circular in nature with an expected associated tendency for instability first following the motion as indeed Fejer has found in such a case.

For the magnetosphere boundary it seems A_1 (on the Earth side) should be expected to be reasonably greater than A_2, so we have not studied these cases in great detail.

In fact it is possible by making a rough estimate of the limiting slope of the common tangent of 1 and 2 when $\phi = 90 - \chi_1$ and $90 - \chi_2$ to put forward a sufficient condition,

$$\frac{A_1 B_1}{A_2 B_2} > 2,$$

for $(\bar{x}_1, \bar{x}_2)$ to remain on 1 for all values of ϕ.

SPECIAL CASE, PARALLEL MAGNETIC FIELDS

When $\chi_1 = \chi_2 \neq 0$, we have the case where in Fig. 6 as θ_1, θ_2 approach 90° sections 1 and 2 tend to the origin simultaneously.

In this case, as might be expected only $U = 0$ gives a stable solution since taking θ arbitrarily close to 90° takes 1 and 2 arbitrarily close to the origin. Clearly unstable modes will first appear propogating nearly perpendicular to the fields, as the stream velocity is increased, for any value of A_1/A_2.

If $\chi_1 = \chi_2 = 0$ the preceding discussion breaks down since $U \cos \phi$ tends to zero as $\bar{x}_1$, $\bar{x}_2$ approach zero. This is a singular case and of little interest physically since the situation could only hold on the magnetosphere boundary at isolated points. It should be noted though that this case is one Fejer has computed with the assumption of identical physical properties on either side.

COMPARISON WITH PREVIOUS PAPERS

We hope to have shown to some extent the relationships between Sen's deduction that the worst perturbation is that propagating perpendicular to the unperturbed field and

Fejer's findings in the cases he studied that unstable modes first occur propagating parallel to the streaming velocity.

When A_1/A_2 is not near unity we have shown the first unstable modes can be expected to be propagating perpendicular to the largest field, provided χ_1 is not too small. When A_1 and A_2 are comparable the critical factor is $\chi_1 - \chi_2$, the angle between the fields, and although we have not studied this case definitively we deduced when $\chi_1 - \chi_2$ is small we expect instability to take place first in modes perpendicular to either A_1 or A_2 and when $\chi_1 - \chi_2$ is nearly a right angle $\tilde{U}(\phi)$ will be more circular in nature and we would expect Fejer's results of instability in modes following the motion.

Both Fejer and Sen mention an upper critical streaming speed which, when exceeded, stabilises the flow. Fejer finds an analytical expression for it in a very particularised case, while Sen gives no expression for it but deduces its existence mathematically. Its existence is suggested by Fig. 5 of this paper, but we feel it has little physical importance in the actual stability problem since, while, for some values of ϕ, $U \cos \phi$ might exceed this speed, it should always be possible to choose a direction with ϕ such that $U \cos \phi$ was greater than $\tilde{U}(\phi)$ but less than this upper critical streaming speed, and so unstable modes would still be present. In any event one would expect the perturbed flow to be non-linear by the time this speed had been attained. We would maintain that whenever $U \cos \phi$ exceeds $\tilde{U}(\phi)$ the flow should be regarded as hydromagnetically unstable.

APPLICATION TO THE MAGNETOSPHERE

As stated before, we can expect over the magnetosphere boundary the Alfven speed on the inside will exceed that on the outside. The actual ratio will vary over the boundary due to the compression effects of the bow shock. Near the sub-solar point the flow will have a stagnation point. Near this point the boundary will be stable with respect to the Kelvin–Helmholtz instability.

In high latitudes the boundary structure might be complicated, particularly if the magnetosphere is open. In such a case the boundary would become diffuse at high latitudes (Dungey, 1967b) and certainly our assumption of negligible boundary thickness could not hold.

Near equatorial regions with either open or closed magnetosphere the boundary should be sharp and therefore the model's application is less doubtful. The most salient feature of our results is our ability to make predictions about the nature of the first unstable modes without a great knowledge of many of the parameters of the problem. On the boundary in low and middle latitudes the flow should have a large component parallel to the equatorial plane (increasing, of course, with decreasing latitude).

The flow velocity then will clearly not be closely aligned to the Earth's field and so as we have shown the stability will be governed by the cusps that occur on the plot of $\tilde{U}(\phi)$. Moving towards dawn or dusk from the noon meridian the flow should be stable until the local conditions are such that (26) is violated. We can make the straightforward deduction from (26) that for southward or northward fields in the magnetosheath (i.e. $\chi_1 = \chi_2$) the entire boundary is unstable hydromagnetically and when the fields are at right angles the boundary is most stable.

We can also from the previous work deduce the nature of the first growing modes. The cusp on $\tilde{U}(\phi)$ occurs when $\chi_1 = 0$ $\chi_2 = |\cos \theta_2| = |\sin (\chi_1 - \chi_2)|$ and so for the first growing modes χ_1 is small and wave fronts will be aligned closely to meridional planes.

We may also investigate the polarisation of these modes. On the Earth side, we know

$$0 < x < \alpha_0 \cos\theta.$$

We are interested in θ near 90°. Clearly we may choose η such that

$$x = \eta\alpha_0 \cos\theta,$$

where

$$0 < \eta < 1.$$

The value of η for a given value of θ will depend on A_1/A_2 (by inspection of Fig. 6).

From Equations (1a) and (2a)

$$\omega B_n^{(1)} = (k_\perp v_\perp^{(1)} + k_n v_n^{(1)})B \tag{29}$$

$$\omega B_\perp^{(1)}, n = -Bk_\parallel v_{\perp,n}^{(1)} \tag{30}$$

$$\rho\omega v_\perp^{(1)}, n = -k_\perp, n\left(p^{(1)} + \frac{BB_\parallel^{(1)}}{\mu}\right) + Bk_\parallel B_{\perp,n}, \tag{31}$$

$$\rho\omega v_\parallel^{(1)} = k_\parallel p^{(1)} \tag{32}$$

where the subscripts $\parallel$, $\perp$, n denote components in plane of the interface parallel and perpendicular to **B** and the component normal to the interface.

(3) gives

$$k_\perp v_\perp^{(1)} + k_n v_n^{(1)} = \frac{\rho^{(1)}\omega}{\rho} - k_\parallel v_\parallel^{(1)}. \tag{33}$$

(33) and (29) give

$$\frac{BB_\parallel^{(1)}}{\mu p} = \left(\frac{1}{a^2} - \left(\frac{Ak_\parallel}{\omega}\right)^2\right). \tag{34}$$

From (31), (30) and (34)

$$\frac{BB_\parallel^{(1)}}{B_\perp^{(1)}} = -\frac{(\omega^2 - (Ak_\parallel)^2)}{k_\parallel k_\perp \left(\frac{1}{a^2} - \left(\frac{k_\parallel}{\omega}\right)^2\right)^{-1} + A^2}$$

which reduces to

$$\frac{B_\parallel^{(1)}}{B_\perp^{(1)}} = -\frac{k_\parallel}{k_\perp} \frac{\left(\left(\frac{\omega}{k_\parallel A}\right)^2 - 1\right)\left(\frac{1}{a^2} - \left(\frac{Ak_\parallel}{\omega}\right)^2\right)}{\left(\frac{1}{\alpha_0{}^2} - \left(\frac{Ak_\parallel}{\omega}\right)^2\right)}. \tag{35}$$

From (32), (30) and (34)

$$\frac{v_\parallel^{(1)}}{v_\perp^{(1)}} = \left(\frac{k_\parallel A}{\omega}\right)\left(\frac{1}{a^2} - \left(\frac{k_\parallel A}{\omega}\right)^2\right) - 1 \frac{B_\parallel^{(1)}}{B_\perp^{(1)}} = \left(\frac{k_\parallel A}{\omega}\right)^2 \frac{((\omega/Ak_\parallel)^2 - 1)}{(1/\alpha_0{}^2 - (Ak_\parallel/\omega)^2)} \frac{k_\parallel}{k_\perp}. \tag{36}$$

By interchanging the subscripts $\perp$ and n one may obtain exactly similar relationships between

$$\frac{v_\parallel^{(1)}}{v_n^{(1)}}, \frac{B_\parallel^{(1)}}{B_n^{(1)}} \quad \text{and} \quad \frac{k_\parallel}{k_n}.$$

We now write

$$k_{\parallel} = k_t \cos\theta$$

$$k_{\perp} = k_t \sin\theta.$$

From (9) k_n and k_t are related by

$$\frac{k_n}{k_t} = i\left(1 - \frac{\eta^4 \alpha_0{}^2 \cos^2\theta}{(1+a^2)(\eta^2-1)}\right)^{1/2}.$$

If, as in the numerical case we computed, we take

$$a^2 = 1/3 \qquad \alpha_0{}^2 = \tfrac{1}{4}$$

and as seems reasonable from the numerical results we take

$$\eta = 0{\cdot}98$$

$$k_n/k_t = i(1 + 10{\cdot}5\cos^2\theta)^{1/2}.$$

So for θ near 90°

$$k_n = ik_t. \tag{37}$$

(36) gives, substituting numerical values,

$$v_{\parallel}^{(1)}/v_{\perp}^{(1)} = 19(k_{\parallel}/k_{\perp}) = 19\cot\theta$$

and also $$v_{\parallel}^{(1)}/v_n^{(1)} = 19(k_{\parallel}/k_n) = -19\,i\cos\theta \text{ using (37).}$$

No (3) gives, using (37)

$$v_{\perp}^{(1)}\sin\theta/v_n^{(1)} + v_{\parallel}^{(1)}\cos\theta/v_n^{(1)} + i = \rho^{(1)}\omega/\rho k_t v_n^{(1)}. \tag{38}$$

From (32)

$$\rho^{(1)} = \rho\omega v_{\parallel}^{(1)}/c^2 k_{\parallel}$$

so that r.h.s. of (38) becomes

$$\frac{\rho^{(1)}\omega}{\rho k_t v_n^{(1)}} = \frac{1}{a^2}\left(\frac{\omega}{Ak_t}\right)^2 \frac{1}{\cos\theta}\frac{v_{\parallel}^{(1)}}{v_n^{(1)}}.$$

So on substitution of numerical values

$$\text{r.h.s. of (38)} = -15\,i\cos^2\theta$$

and thus when θ is near 90° from (38) $v_t^{(1)} = -iv_n^{(1)}$, where

$$v_t^{(1)} = v_{\perp}^{(1)}\sin\theta + v_{\parallel}^{(1)}\cos\theta$$

denotes the component of $\mathbf{v}$ parallel to $\mathbf{k}_t$
also

$$\text{div}\,\mathbf{B}^{(1)} = 0$$

gives

$$B_t^{(1)} = -iB_n^{(1)}$$

from (37). From (35) substituting numerical values

$$\left|\frac{B_{\parallel}^{(1)}}{B_{\perp}^{(1)}}\right| = |5\cot\theta|$$

and

$$\left|\frac{B_{\parallel}^{(1)}}{B_n^{(1)}}\right| = |5\cos\theta| \qquad \text{near } \theta^\circ = 90$$

and so for θ near 90° we have a circularly polarised disturbance with disturbance vectors closely aligned to a plane perpendicular to the Earth's field.

We have thus found the nature of the first growing modes. This clearly bears out Atkinson and Watanabe's speculation (1966) about the form of modes originating on the boundary due to the Kelvin–Helmholtz instability. They used a physical argument and deduced the existence of circularly polarised disturbances on field lines near the boundary which they suggested would propagate along the field lines to the Earth. On this assumption they suggested expected periods would be in the pc 5 range. The problem of how the disturbances we have found propagate to Earth has yet to be studied in a non-uniform field. The polarisation though will be consistent with that observed for pc 2–5 and pi 2 pulsations (Troitskaya 1967).

We might expect intuitively the disturbance to propagate to Earth in some form of guided mode and so from (37) we must expect the associated disturbance to be heavily attenuated in latitude. This is born out in a large number of cases for pulsations (Troitskaya, 1967). Ionospheric effects might cause some spread in latitude though.

Until a model of propagation to Earth has been developed we cannot make predictions about the actual expected frequencies. It should be noted though that we have here a natural hydromagnetic explanation of circular polarisation for disturbances with expected frequencies much less than the proton gyrofrequency without invoking the Hall effect.

CONCLUSION

We have in this fuller treatment of the Kelvin–Holmholtz instability in infinitely conducting compressible fluids brought out significant features of the problem which have not been mentioned in previous treatments.

To some extent we hope to have shown the relationship between Fejer's and Sen's differing conclusions in their previous treatments of the problem.

The most important feature is that if the Alfven speed on one side of the boundary is significantly greater than that on the other side, the form and direction of the first growing modes is relatively independent of the direction of the streaming velocity provided it is not too closely aligned to the field with larger Alfven speed. This, as applied to the magnetosphere boundary, gives a mechanism for the production of circularly polarised hydromagnetic waves at the boundary.

The problem of how the waves develop as one moves towards dawn or dusk boundaries has not been studied. We must expect though that the dawn and dusk boundaries experience heavy instability as has been suggested by OGO 1 observations (Heppner *et al.*).

Acknowledgement—I would like to thank Professor J. W. Dungey for both suggesting the problem and for many subsequent helpful discussions.

REFERENCES

ATKINSON, G. and WATANABE T. (1966). Surface waves on the magnetosphere boundary as a possible origin of long period micropulsations, *Earth Planet Sci. Lett.* **1**, (2), 89.

DUNGEY J. W., (1967a). The theory of the quiet magnetosphere, in *Solar Terrestrial Physics*, p. 91. Academic Press, London.

DUNGEY J. W. (1967b). The reconnection model of the magnetosphere, to be published in Proc. NATO Advanced Study Institute, *Earth's Trapped Radiation* (Ed. B. M. McCormac).

FEJER, J. A. (1964). Hydromagnetic stability at a fluid velocity discontinuity between compressible fluids, *Phys. Fluids* **7**, 499.
HEPPNER, J. P., SUGIURA M., SKILLMAN T. L., LEDLEY B. G. and CAMPBELL M. (1967). OGO-A magnetic field observations, Goddard Space Flight Center, *NASA* Report X-612-67-150.
LERCHE, I. (1966). Validity of the hydromagnetic approach in discussing instability of the magnetospheric boundary, *J. geophys. Res.* **71**, (9), 2365.
SEN, A. K. (1965). The stability of the magnetospheric boundary, *Planet. Space Sci.* **13**, 131.
TROITSKAYA, V. A. (1967). Micropulsations and the state of the magnetosphere, in *Solar Terrestrial Physics*, p. 213. Academic Press, London.

APPENDIX

Validity of assuming $r(\phi)$ is a lower bound of $\tilde{U}(\phi)$

Our assumption is equivalent to requiring that the family of lines

$$A_1 x_1 + A_2 x_2 = U \cos\phi,$$

with U increasing passes through $(\alpha_1, \cos\theta_2)$ prior to being tangential to section 1 in Fig. 6.

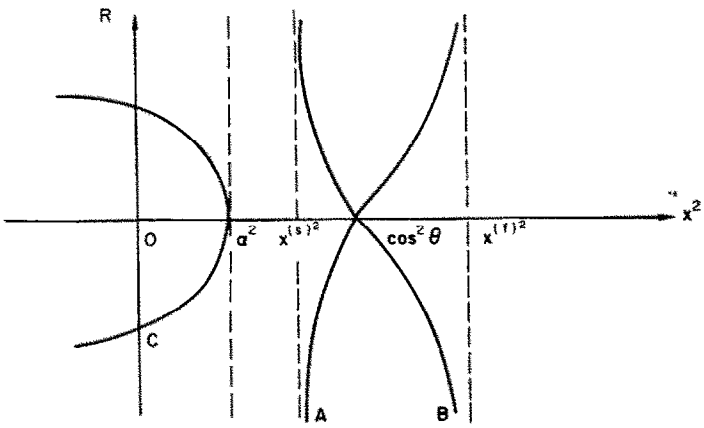

FIG. 10. PLOT OF $\pm(x^2 - \cos^2\theta)\left(\dfrac{\alpha^2 - x^2}{(x^2 - x^{(s)^2})(x^2 - x^{(f)^2})}\right)^{1/2}$ AGAINST x^2.

We require this for all values of A_1/A_2 and a sufficient condition for this to be so is that there are no points of inflexion on 1.

On $$F(x_1, x_2) = 0$$

$$\frac{dx_2}{dx_1} = -\frac{D_1 R_1}{D_2 R_2} \text{ from (22)},$$

where D_1, D_2 represent differentiation with respect to x_1, x_2 respectively.

Therefore

$$\frac{d^2 x_2}{dx_1^2} = -\frac{D_1^2 R_1 (D_2 R_2)^2 + D_2^2 R_2 (D_1 R_1)^2}{(D_2 R_2)^3}. \tag{A1}$$

For no points of inflexion this must not change sign on section 1.

It is adequate for our purposes here to write:

$$R = \frac{x^2 - \cos^2\theta}{y}$$

$$y = \sqrt{\left(\frac{(x^2 - x^{(s)^2})(x^2 - x^{(f)^2})}{(\alpha^2 - x^2)}\right)}.$$

These differ from the previous definitions purely by proportionality factors. A sketch of

$$(x^2 - \cos^2\theta)\sqrt{\left(\frac{\alpha^2 - x^2}{(x^2 - x^{(s)^2})(x^2 - x^{(f)^2})}\right)}$$

is given in Fig. 10 as a function of x^2. Section A and the lower half of C form R in this graph.

Any straight line will intersect with the curve in up to 4 places. We may therefore conclude that on branch A there is only one point of inflexion and branch C may contain none.

We may therefore conclude when $0 < x_1 < \alpha_1$

$$\frac{dR_1}{d(x_1^2)} > 0 \quad \text{and} \quad \frac{d^2R_1}{d(x_1^2)^2} > 0.$$

Now

$$D_1R_1 = 2x_1 \frac{dR_1}{d(x_1^2)}$$

and

$$D_1^2R_1 = 2\frac{dR_1}{d(x_1^2)} + 4x_1^2 \frac{d^2R_1}{d(x_1^2)^2}$$

and so $D_1R_1 > 0$ and $D_1^2R_1 > 0$ in the required interval.

For $x_2 > \cos\theta_2$ clearly D_2R_2 will be positive since by inspection of Fig. 10 it may have no roots between $\cos\theta_2$ and $x_2^{(f)}$.

From (A1) d^2x_2/dx_1^2 may only be positive if at some point on 1

$$D_2^2R_2 < 0 \tag{A2}$$

and

$$\left|\frac{D_1^2R_1}{D_2^2R_2}\right| < \left(\frac{D_1R_1}{D_2R_2}\right)^2. \tag{A3}$$

Now

$$\frac{dR}{dx} = \frac{2x}{y} - \frac{R}{y}\frac{dy}{dx}$$

and

$$\frac{d^2R}{dx^2} = \frac{2}{y} - \frac{2x}{y^2}\frac{dy}{dx} - \frac{dR}{dx}\frac{dy}{dx}\frac{1}{y} - \frac{R}{y^2}\frac{dy}{dx} - \frac{R}{y}\frac{d^2y}{dx^2}$$

and since $y(\cos\theta) = (1 + a^2)^{1/2}\sin\theta$ and

$$\frac{dy}{dx}(\cos\theta) = 2\cot\theta(1 + a^2)(a^2 - 1)$$

$$\frac{d^2R}{dx^2}(\cos\theta) = \frac{2}{(1 + a^2)^{1/2}\sin\theta}(1 - 4\cot^2\theta(a^2 - 1)).$$

Therefore (A2) may be fulfilled if and only if

$$\tan^2\theta < 4(a^2 - 1) \tag{A4}$$

therefore if $a_2^2 < 1$ (A2) cannot hold and our assumption is valid.

(A4) is a condition for $D_2^2 R_2$ to be negative at $x_2 = \cos\theta_2$. As x_2 approaches $\cos\theta_2$, x_1 approaches α_1 and so the l.h.s. of (A3) is proportional to $(\alpha_1^2 - x_1)^{-3/2}$ and the r.h.s. is is proportional to $(\alpha_1^2 - x_1^2)^{-1}$. So we must assume

$$\theta_2 \ll \tan^{-1} 2\sqrt{(a^2 - 1)}$$

if (A3) is to hold at a point near $(\alpha_1, \cos\theta_2)$ since $D_2^2 R_2$ must not be small.

At the other end of the interval, near $(0, \xi_2)$ $D_1 R_1$ tends to zero while $D_2 R_2$, $D_1^2 R_1$, $D_2^2 R_2$ remain finite so (A3) is unlikely to hold.

It is clear then our assumption may only come into doubt when θ_2 is small. If θ_1 is also small this is not important. On the other hand if θ_1 is large (i.e. $\chi_1 - \chi_2 \sim 90°$) care should be excerised in use of (26) although only a small range of A_1/A_2 should be affected and since we may expect the point of inflexion to be near $(\alpha_1, \cos\theta_2)$ the estimate given by (26) should not be far wrong.